energies

MDPI

Article

Research and Development of the Oxy-Fuel Combustion Power Cycle for the Combined Production of Electricity and Hydrogen

Vladimir Kindra *, Andrey Rogalev, Maksim Oparin, Dmitriy Kovalev and Mikhail Ostrovsky

Moscow Power Engineering Institute, National Research University, Krasnokazarmennaya, 14, 111250 Moscow, Russia; rogalevan@mpei.ru (A.R.); oparinmv@mpei.ru (M.O.); kovalevds@mpei.ru (D.K.); ostrovskyma@mpei.ru (M.O.)

* Correspondence: kindra.vladimir@yandex.ru

Abstract: Modern trends in improving environmental safety have determined the urgency in creating innovative technologies that allow the production of electricity and hydrogen without the emission of harmful substances. However, at the moment, there are not so many technical solutions offering the combined production of these useful products with a high degree of efficiency and environmental friendliness. The transition to oxy-fuel combustion power cycles for the co-production of electricity and hydrogen is a prospective way to decrease carbon dioxide emissions into the atmosphere from the energy sector. To achieve zero emissions, the semi-closed oxy-fuel combustion cycle is combined with a steam methane reformer, which has a high energy efficiency through reducing losses in the steam turbine condenser. The modeling methodology has been described in detail, including the approaches to defining the working fluid properties and mathematical models of the different steam methane reforming plants and the oxy-fuel combustion power plant. According to the results of the thermodynamic analysis of the steam methane reforming plant, it was found that an increase in the temperature from 850 to 1000 °C leads to a decrease in the mass flow fuel by 16.3% due to the shift towards a direct reaction. Moreover, the optimal temperature in the reformer lies in the range of 900–950 °C. A comparison of the energetic and ecological characteristics of various steam methane reformer units showed that the scheme with oxy-fuel combustion is better compared to the scheme with CO_2 capture by absorption in monoethanolamine; the efficiency is 6.9% higher and emissions of carbon dioxide are 22 times lower. According to the results of the thermodynamic analysis of a novel oxy-fuel combustion power cycle, it was found that its performance varied regarding the range of electricity production (123.6–370 MW) and hydrogen production (0–10.8 kg/s). The efficiency of the oxy-fuel combustion power cycle varies in the range of 47.2–70.1%. Based on the results of the operation regimes analysis, the energy complex performance map has been developed, allowing identification of the efficiency and working fluid massflow by net power and produced hydrogen massflow.

Keywords: carbon dioxide; oxygen; efficiency; steam methane reforming; gas turbine; heat exchanger; net zero emission; power generation

Citation: Kindra, V.; Rogalev, A.; Oparin, M.; Kovalev, D.; Ostrovsky, M. Research and Development of the Oxy-Fuel Combustion Power Cycle for the Combined Production of Electricity and Hydrogen. *Energies* **2023**, *16*, 5983. https://doi.org/10.3390/en16165983

Academic Editor: Jaroslaw Krzywanski

Received: 6 July 2023
Revised: 11 August 2023
Accepted: 13 August 2023
Published: 15 August 2023

1. Introduction

1.1. The Relevance of the Decarbonization of Electricity and Hydrogen Production

The continuous growth of the population and the active industrialization of countries are the reasons for the significantly increasing demand for energy products, both electricity and hydrogen. This is evidenced by the data of the Centre for Energy Economics Research and Policy [1], according to which from 2020 to 2050, the demand for electricity will increase by more than 160% and the demand for hydrogen by 246%. Taking into account the identified trend towards the growth in energy production, one should expect an increase in emissions of toxic substances and greenhouse gases into the atmosphere.

The concern of the global community with regards to global climate change has led to the adoption of a number of international treaties mandating countries to stabilize or reduce greenhouse gas emissions by reforming their energy sectors. In particular, in 1997, the Kyoto Protocol was signed, and in 2015, the Paris Agreement. However, to achieve the desired effect of reducing CO_2 emissions, relevant agreements need to be adopted by the largest industrial nations [2].

Decarbonization of the energy industry is one of the key challenges on the way to achieving carbon neutrality [3]. In addition to electric energy, steam, and hot water, hydrogen is another energy product that is in high demand. It is employed across numerous industries. In particular, hydrogen fuel is used in oil refining, metallurgy, and the construction and food industry. In addition, hydrogen is used as a fuel in engines and in standalone power and heat generators; it is a convenient medium to supply heat to distributed consumers, and to transport and store energy [4,5]. An important advantage of hydrogen is its environmental safety; the sole product of its combustion is water vapor. However, since pure hydrogen is almost never found in nature, it needs to be produced first, and the method of its production will largely determine the environmental effect of its use [6,7].

Specifically, approximately 48% of hydrogen is produced by conversion [8]. The conversion of gases involves processing them to change the composition of the initial gas mixture. The conversion is normally applied to hydrocarbon gases (methane and its homologues) and carbon monoxide to produce hydrogen or a mixture of hydrogen and carbon monoxide. The conversion process is carried out using various oxidizing reagents (such as oxygen, steam, CO_2, and mixtures thereof).

The most cost-efficient feedstock for conversion is methane (natural gas). Currently, the majority of the industrially produced hydrogen is generated using the steam methane reforming (SMR) process. However, the carbon dioxide formed during the SMR process is not captured and is released into the atmosphere. Such hydrogen is referred to as "gray" hydrogen. To ensure that this process is environmentally neutral, one needs to additionally apply the carbon capture and storage technologies; however, their addition results in the process being considerably more expensive. On average, the cost of SMR production of "blue" hydrogen is 23% higher than that of "grey" hydrogen [9]. The above considerations result in the development of an environmentally safe and economically viable SMR-based hydrogen production process being a high-priority objective.

1.2. Reducing Carbon Dioxide Emissions from the Steam Methane Reforming Plants

In the SMR process, steam reacts with natural gas at high temperatures and moderate pressure (1.5–2 kgf/cm^2) in the presence of a nickel-containing catalyst (up to 20% Ni as NiO). Steam and thermal energy are needed to separate the hydrogen from the methane carbon base.

SMR is currently the cheapest (and most mastered) process for the industrial production of hydrogen. However, it is accompanied by CO and CO_2 emissions. There are various solutions available to handle those emissions.

The International Energy Agency (IEA) has provided comparative analysis data for different versions of the combined hydrogen, heat, and electricity generation process in its publication [10], where emerging SMR process configurations are examined alongside their feasibility analysis. The publication has identified several methods of CO_2 capture: (a) a method based on chemical absorption technology; (b) a method based on introduction of burners running on H_2-saturated fuel; and (c) a method based on low-temperature separation of CO_2 and the application of membrane technology.

It should be noted that in SMR plants, three areas are identified where CO_2 can be captured: (1) from the syngas stream downstream the water–gas shift reactor; (2) from the tail gas stream of the PSA (pressure swing adsorption) unit; and (3) from SMR flue gases [11].

Obviously, the most efficient option for a SMR unit is the one without any CO_2 capture systems, and in the complete absence carbon emissions control, there is no reason to implement such systems.

The introduction of a system for capturing CO_2 from the syngas stream using a chemical absorption process results in a 54% reduction in CO_2 emissions compared to the version without the capture. Adding the H_2-saturated fuel fed to the burners of the reformer furnace further increases the share of prevented CO_2 emissions to 64% [12].

There are versions of the process involving purification of the tail gases from the PSA unit. The introduction of capture systems based on chemical absorption technology leads to a reduction in CO_2 emissions by 52%, and the introduction of systems based on low-temperature separation of CO_2 and the application of membrane technology by 53%. The latter option has been noted to be most effective in the partial implementation of carbon border adjustment [13].

With the full implementation of the carbon border adjustment mechanism, the most efficient option is an SMR unit with CO_2 capture from SMR flue gases. The introduction of such a capture system can reduce emissions by as much as 90% [10].

Therefore, most of the known SMR-based hydrogen production processes with minimum greenhouse gas emissions result either in an increase in the present value of hydrogen production by 44% for the most efficient capture option, or in a low percentage of CO_2 capture for other options. This means that the development of a highly efficient SMR technology with minimal emissions of harmful substances is a high-priority objective.

1.3. Oxy-Fuel Combustion Technology for the Combined Production of Electricity and Hydrogen

Today, the main global trend in the development of energy is to reduce the number of toxic substances and greenhouse gases emissions into the atmosphere. Much research has been devoted to investigating the issue of reducing emissions of harmful substances from the power generation units [14–19]. Many emission reduction methods are successfully used at the existing thermal power plants. In particular, methods of controls of atmospheric pollutants, such as nitrogen and sulfur oxides, are widely used. At the same time, the prevention of carbon dioxide emissions, which are formed in large quantities during the combustion of fossil fuels, still causes difficulties. The introduction of carbon dioxide capture technologies leads to a significant increase in the electricity cost; therefore, the issue of creating environmentally friendly and economically viable high-capacity energy systems remains open [20,21].

Oxy-fuel energy complexes with a CO_2 working flow have great potential as a way of reducing emissions while maintaining a high level of thermal efficiency. Oxy-fuel technologies for power generation are based on the combustion of hydrocarbon fuels in pure oxygen and the capture of carbon dioxide and its disposal. Currently, more than thirty cycles with oxygen fuel combustion are known [22–24]. In particular, the following closed thermodynamic cycles are widely known: SCOC-CC, MATIANT cycles, NET Power cycles, Graz cycles, CES cycles, AZEP cycle, and ZEITMOP [25].

The initial versions of such cycles were introduced at the end of the past century. Today, the US, Japan, and European countries are actively developing this avenue. Due to the allocation of grants, active subsidization of “green” technologies for power generation, and the establishment of legislative frameworks facilitating the reduction of CO_2 emissions, scientific research is being conducted, experimental plants are being built, and prerequisites are being created for building actual power units with “zero” emission of harmful substances. Large energy corporations are joining their efforts to build demo plants capable of releasing up to 50 MW of electricity to the power grid [26].

Recent developments in the field of creating environmentally friendly energy complexes are aimed at creating power units that simultaneously generate both electric power and hydrogen. Such solutions can simultaneously produce two important energy products at high efficiency rate and without harmful emissions.

In particular, in the work of Zhang N. [27], two novel system configurations were proposed for oxy-fuel natural gas turbine systems with integrated steam reforming and carbon dioxide capture and separation. The steam reforming heat is obtained from the available turbine exhaust heat, and the produced syngas is used as fuel with oxygen as

the oxidizer. The authors were focused on the integration of the turbine exhaust heat recovery with both reforming and steam generation processes, in ways that reduce the heat transfer-related exergy destruction. According to the modeling results, a net efficiency of power generation unit is in the range of 50–52%. The key disadvantage of the proposed configuration is the losses occurring in the condenser and the performer.

The article [28] presents a combination of CCGT with steam conversion of methane; however, the reformer is used in this cycle as a method of producing fuel for the power unit. To purify the outgoing gases from the reformer from carbon dioxide, an installation with monoethanolamine is used, which allows the generation of electricity without emissions, with an efficiency of 41.77%. The disadvantage of this technology is the lack of the possibility of producing hydrogen for sale to an external consumer, large heat losses in the condenser of the steam turbine unit and outgoing gases, and large expenses for cleaning carbon dioxide at the outlet of the methane steam conversion plant.

In the work [29], an oxy-fuel combustion power plant for electricity and hydrogen production is presented with near-zero emissions. It represents the combination of two technologies: the Allam cycle and the steam methane reforming plant. According to the modeling results, the power plant efficiency is 54.9% at equal production of the supplied electricity and chemical energy of the produced hydrogen. The absence of a water steam source in the Allam cycle thermal loop is one of the key issues that one faces when trying to integrate a steam methane reformer into the process. It necessitates the supply of low-grade heat to the multi-flow regenerator, which further complicates the issue of controlling the output of electricity and hydrogen in the course of the combined production of energy products.

The above issue can be solved by creating an oxy-fuel energy complex for zero-emission electricity and H_2 production based on the SCOC-CC cycle. The fact that this configuration includes a steam turbine circuit results in it being possible to draw steam from its individual branches, which should considerably simplify the load control issue. Moreover, the solution allows an increase in the combined unit efficiency. However, in open sources, no references are available to the results of studies on the energy performance and modes of operation of such power units. Therefore, this paper presents the results of the research and the development of a novel oxy-fuel combustion power cycle for the combined production of electricity and hydrogen. Special attention is paid to the thermodynamic analysis of the oxy-fuel combustion SMR and power plants.

2. Research and Development of the Steam Methane Reforming Plant with Oxy-Fuel Combustion

2.1. Existing and Promising Technological Schemes in the Steam Methane Reforming Plants

The object of the research are three technological schemes in the steam methane reforming plants:

- Scheme of the steam methane reforming plant without CO_2 capture (Figure 1);
- Scheme of the steam methane reforming plant with CO_2 capture by absorption in MEA (Figure 2);
- Scheme of the steam methane reforming plant with oxy-fuel combustion and CO_2 capture (Figure 3).

Figure 1 shows a scheme of a steam methane reformer. The methane stream (1) enters the gas booster compressor (GBC) and is compressed to a pressure of 20–25 bar and is then mixed with water steam (17). The steam–gas mixture (4) enters the high-temperature steam reformer. Fuel methane gas (3), tail gas (10), and air (12) are fed to the burners of the reformer furnace. In the steam reformer, in the presence of a nickel catalyst and at a temperature of approximately 900 °C, syngas (5) is formed, which consists of hydrogen, carbon dioxide, and carbon monoxide. Syngas undergoes water cooling in HE_1 and enters the high-temperature water–gas shift reactor, where, due to catalytic reaction with steam, the hydrogen content in the gas is increased, after which, as a result of additional cooling in HE_2, it becomes possible to remove the excess moisture (16) from the syngas in the

cooler/separator. H_2-enriched syngas enters the pressure swing adsorber, where it is purified from carbon dioxide, carbon monoxide, and methane, producing pure hydrogen. The tail gas is mixed with the methane stream (3) at the inlet to the reformer furnace burners.

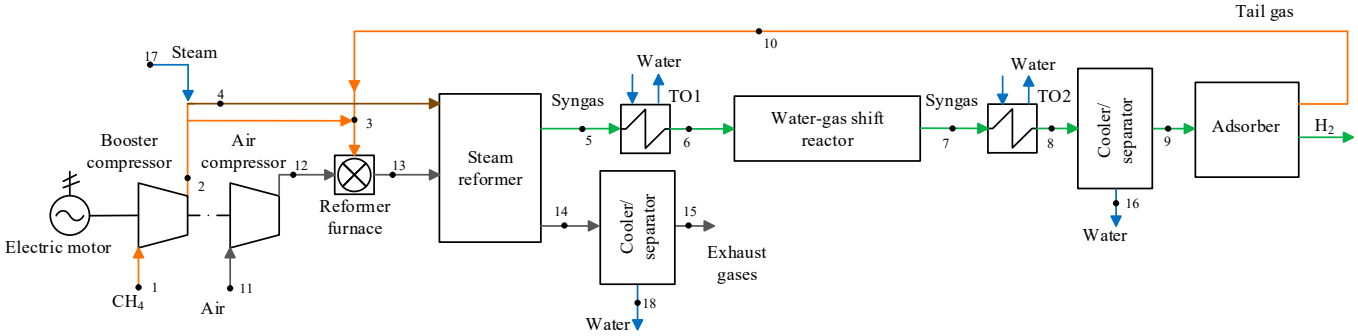

Figure 1. Scheme for the steam methane reforming plant without CO_2 capture.

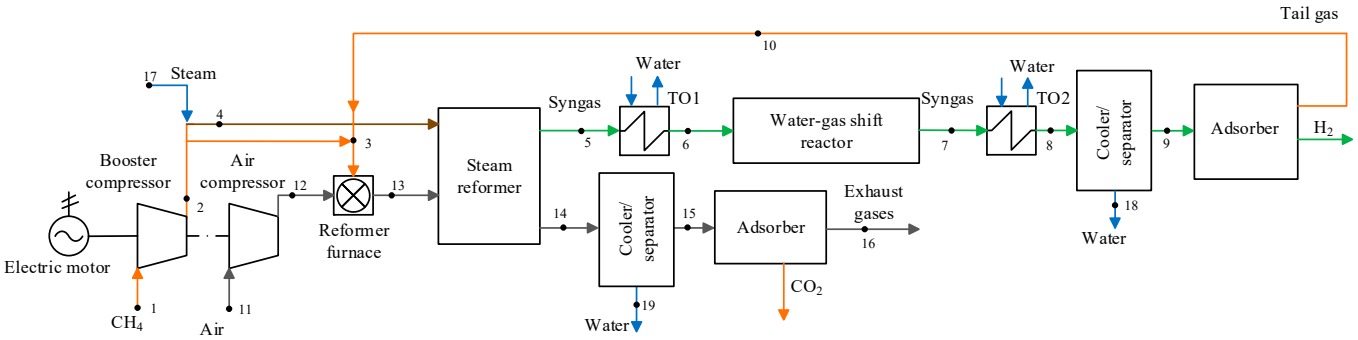

Figure 2. Scheme for the steam methane reforming plan with CO_2 capture.

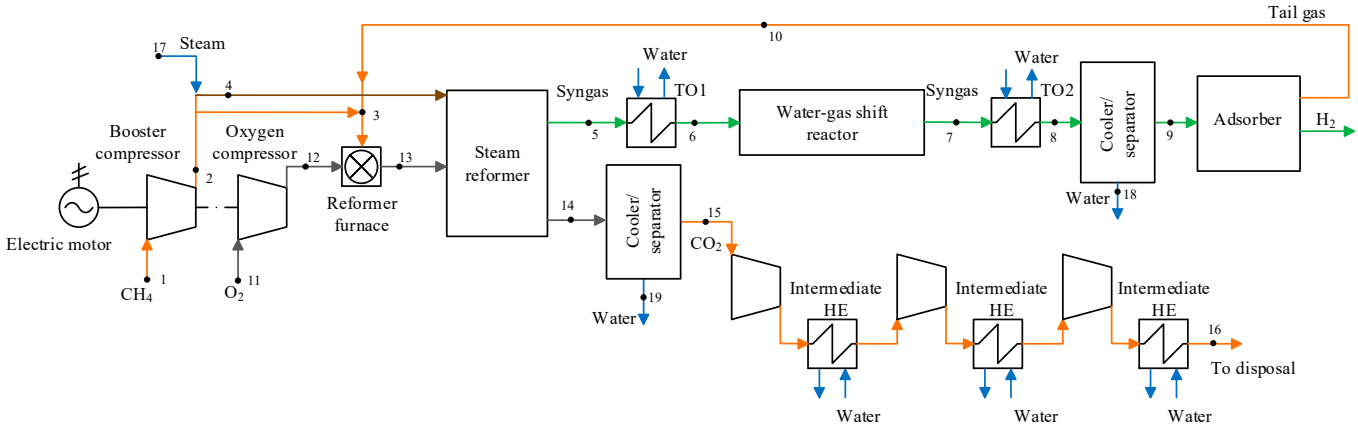

Figure 3. Scheme for the steam methane reforming plant with oxy-fuel combustion and CO_2 capture.

The key disadvantage of this configuration is the high level of flue gas emissions from the high-temperature steam reformer. To lower it, a configuration of methane reformer with flue gas purification is traditionally used (Figure 2), with the main distinction of this configuration from the basic one being the presence of a cooler/separator and an adsorber unit for the adsorption of flue gases from the high temperature steam reformer (14). This kind of configuration considerably increases the final cost of the hydrogen produced.

This paper proposes a configuration of the steam reforming process with oxy-fuel combustion (Figure 3) [30], the key feature of which is the use of pure oxygen (11) as an oxidizer for fuel combustion. As a result, the flue gases of the high-temperature steam reformer contain only water vapor and carbon dioxide. This solution results in it being possible to completely remove moisture (19) from the flue gases (14) in the cooler/separator

and to compress pure carbon dioxide (15) in a multi-stage compressor with intercooling, which is sent for disposal (16).

2.2. Mathematical Models of the Steam Methane Reforming Plants

Process flow modeling for SMR units was performed in Aspen Plus [31], the software solution widely applied for calculation of processes in the petrochemical industry and frequently used for building the models of carbon dioxide capture units. Thermophysical properties of substances were determined using the NIST Refprop database [32]. Table 1 contains the summary of input data for the SMR mathematical model.

Table 1. Performance characteristics for modeling steam methane reformers.

Characteristics	Value
Ambient pressure, bar	0.1
Ambient temperature, °C	15
Fuel temperature, °C	20
Fuel pressure, bar	7
Fuel	100% CH_4
Lower heating value for CH_4 (at 15 °C and 7 bar), kJ/kg	50
Lower heating value for H_2 (at 15 °C and 7 bar), kJ/kg	130
Inlet pump temperature, °C	15
Compressor isentropic/mechanical efficiency, %	85/99
Pump polytropic/mechanical efficiency, %	75/99
CO_2 compressor/turbine polytropic efficiency, %	85/99
Pinch point temperature in the heater, °C	5
O_2 purity, %	95.6
Reformer pressure, MPa	2
ASU delivery pressure, bar	11
ASU delivery temperature, °C	30
Specific energy consumption for the production of 1 kg of oxygen, kW/kg O_2	1.093

While modeling the SMR units, the stoichiometric process of oxygen combustion in the reformer furnace was considered. The oxy-fuel combustion process is presented in Formula (1):

$$CH_4 + 2 \cdot O_2 = 2 \cdot H_2O + CO_2 \quad (1)$$

Inside the reformer shown in Figure 4, the reaction of methane oxidation by steam and the water–gas shift reaction occurs, which are calculated using Formulas (2) and (3). In turn, the reactions occurring in the high-temperature CO conversion reactor proceed as expressed by Formula (3):

$$CH_4 + H_2O \leftrightarrow CO + 3H_2;\ \Delta H_0 = 206.2 \frac{kJ}{mole} \quad (2)$$

$$CO + H_2O \leftrightarrow CO_2 + H_2;\ \Delta H_0 = -41.2 \frac{kJ}{mole} \quad (3)$$

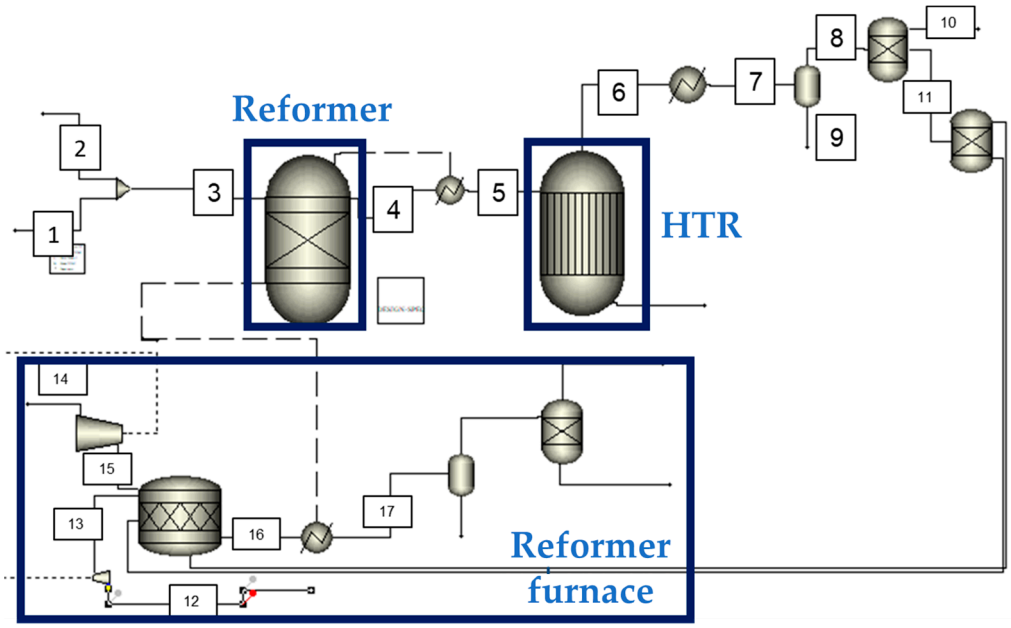

Figure 4. Mathematical model of a methane steam reformer.

When modeling the steam methane reformer, the following assumptions were generated:

1. Stoichiometric fuel combustion;
2. Zero pressure loss in pipelines;
3. No nitrogen oxides formed during combustion;
4. Energy losses during mixing of methane and steam were not considered.

The model of the absorber plant is shown in Figure 5; it includes an absorption column, a regeneration column, a waste heat exchanger (WHE), rich and regenerated amine pumps, an air blower, a cooler, and a separator for separating the liquid phase from the carbon dioxide stream. The flue gases entering the plant are forced into the bottom of the absorption column by the air blower. The amine solution and make-up water are fed to the top of the column. Next, going up the absorption column, the gas is washed with the amine solution, which absorbs carbon dioxide. The purified gas exits from the top of the column, while the rich amine solution flows to its bottom. The rich amine solution then enters the pump, which feeds it to the waste heat exchanger. In the WHE, the rich amine solution is warmed up by the regenerated amines and then enters the top of the regeneration column. There, the amine solution flows down, and CO_2 is separated from it. The bottom of the column is provided with a reboiler that evaporates the solution and supplies heat for the separation process. A condenser is installed at the top of the regeneration column; it cools down the stream and separates the vapors from the condensate, which flows back into the column. Next, the stream is cooled down again and is separated in the separator, after which the CO_2-rich vapors are removed, and the condensate is fed to the inlet of the regenerated amine pump. The regenerated amine solution downstream of the reboiler enters the hot side inlet of the waste heat exchanger, and after cooling, it enters the inlet of the regenerated amine pump, and a make-up amine solution is also fed there. For the parameters of the stream purified by amine washing, refer to Table 2.

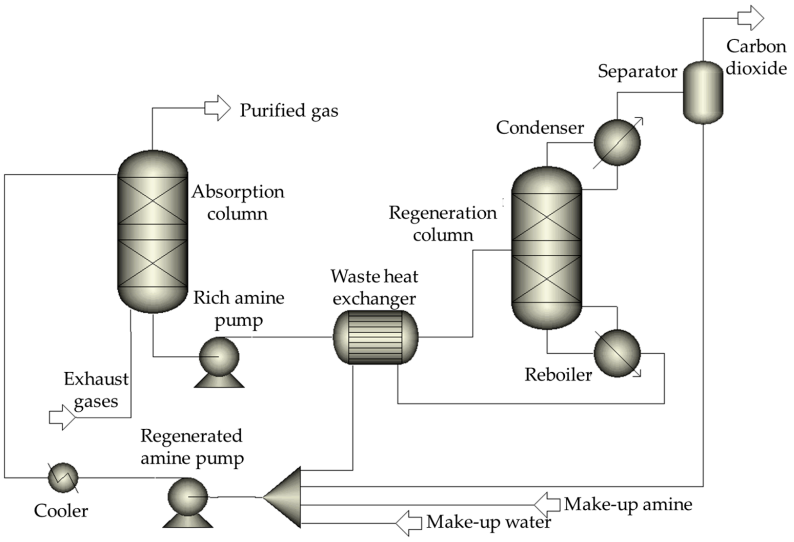

Figure 5. Model of an absorption plant in Aspen Plus.

Table 2. Exhaust gases flow parameters.

Characteristics	Units	Value
Temperature exhaust gases	°C	90
Pressure exhaust gases	bar	1
Mass flow flue gas	kg/s	1
Mass fraction CO_2	%	2.60
Mass fraction H_2O	%	2.13
Mass fraction O_2	%	19.29
Mass fraction N_2	%	75.98

The parameters in Table 3 served as input data for modeling the plant for absorption purification with the 30% MEA solution (Figure 5).

Table 3. Input data for the calculation of the carbon dioxide capture plant.

Characteristics	Units	Value
Outlet heat exchanger temperature	°C	80
Outlet separator temperature	°C	30
Outlet regenerated amine pump pressure	bar	1.08
Outlet saturated amine pump pressure	bar	1.1
Absorber column parameters		
Number of stages	pc	15
Additional water supply per stage	pc	1
Flue gas supply to the stage	pc	15
Supply of regenerated amine	pc	2
Pressure in the first stage	bar	1
Stage pressure loss	bar	0.05
Recovery column parameters		
Number of stages	pc	15
Carbon dioxide removal	pc	1
Withdrawal of regenerated amine	pc	15
Saturated amine feed	pc	3
Pressure in the first stage	bar	1
Stage pressure loss	bar	0.05
Reflux fraction in the condenser	-	0.5
Reboiler share	-	0.7

Since simulation of the SMR processes for hydrogen production consumes electrical energy to maintain the operation of the primary and auxiliary equipment, the fuel heat utilization factor (HUF) calculated using Formula (4) was used as the main indicator of their energy efficiency:

$$\mathrm{HUF} = \frac{G_{\mathrm{H_2}} \cdot Q^h_{l_{\mathrm{H2}}} - \frac{N_{o.n.\ MSR} + N_{capt.MSR} + N_{storage}}{\eta_{elect.}}}{B \cdot Q^h_{l_{\mathrm{CH4}}}} \quad (4)$$

where $G_{\mathrm{H_2}}$ is the hydrogen mass flow, kg/s;

$Q^h_{l_{\mathrm{H2}}}$ is the lower heating value for H_2, MJ/kg;

$N_{o.n.\ MSR}$ is the energy cost for own needs of the methane steam reformer, MW;

$N_{capt.MSR}$ is the energy costs for CO_2 capture, including energy costs for O_2 production in ASU, MW;

$N_{storage}$ is the energy costs for carbon dioxide storage, MW;

B is the methane mass flow, kg/s;

$Q^h_{l_{\mathrm{CH4}}}$ is the lower heating value for CH_4, MJ/kg;

$\eta_{elect.}$ is the efficiency of electricity production spent for the own needs of the SMR (assumed to be 43%) [33].

To verify the modeling results, a comparison with the data presented in [34] was performed. According to the modeling results, at a temperature and pressure at the outlet of the reformer equal to 700 °C/40 bar, the maximum error is achieved in the volume composition of the carbon dioxide mixture equal to 0.645%. The results of the verification are shown in Table 4.

Table 4. Verification results.

Characteristics	Value		Error, %
Temperature, °C	700		
Pressure, bar	40		
H_2O/CH_4 ratio	3		
Composition (vol%)	Math. model	Fahim M. A. At at	
CH_4	13.2	13.13	0.530
CO	9.9	9.85	0.505
CO_2	9.3	9.36	0.645
H_2	67.6	67.66	0.089

2.3. Thermodynamic Analysis of the Steam Methane Reforming Plants

To identify the most energy-efficient version of the steam reformer, thermodynamic optimization of the two cycles was performed. When modeling SMR units producing 1 kg of hydrogen, the temperature of the steam reforming products downstream of the reformer was changed from 850 °C to 1000 °C in 50 °C increments. Over the course of this temperature increase in the reformer, one can observe the correlations described by the Le Chatelier's principle for the methane reforming Equation (3). As the temperature grows, the pressure decreases, and the H_2O/C ratio in the initial mixture increases, the chemical equilibrium of the reaction will shift towards a direct reaction. This causes the total fuel consumption for production to decrease by 0.43 kg/s relative to the production of hydrogen at 850 °C (Figure 6a).

However, the thermal power consumed by the reformer increases by 4 MW, which causes an increase in the methane consumption in the combustion chamber by 0.35 kg/s (Figure 6b). The change in the total fuel consumption is shown in Figure 6c. It should be noted that the difference in fuel consumption in the SMR processes with air combustion and oxygen combustion is due to the air and CO_2 compressors operating in different conditions; in the first case, the process occurs at the initial atmospheric pressure, and in the second case, it unfolds within a semi-closed cycle, so the compressor is installed to compensate for the hydraulic losses taking place in the reformer.

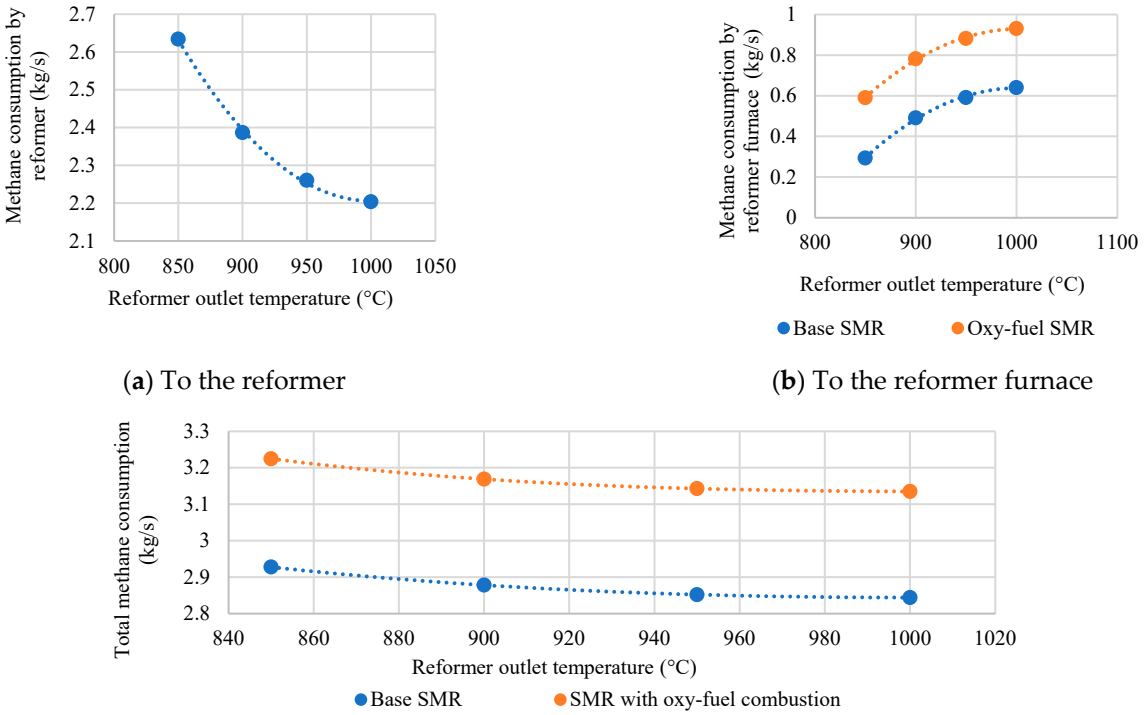

(**a**) To the reformer

(**b**) To the reformer furnace

(**c**) Total consumption of methane in SMR

Figure 6. Consumption of methane in SMR.

In the course of the analysis, the optimal reaction temperature in the reformer was determined to be 950 °C (Figure 7). Any further temperature increase does not cause any significant reduction in the consumption of methane per 1 kg of hydrogen produced (it decreases by 0.06 kg/s). This is due to the fact that when the steam methane reforming limit is reached, the excess heat is mainly consumed by heating the reaction products.

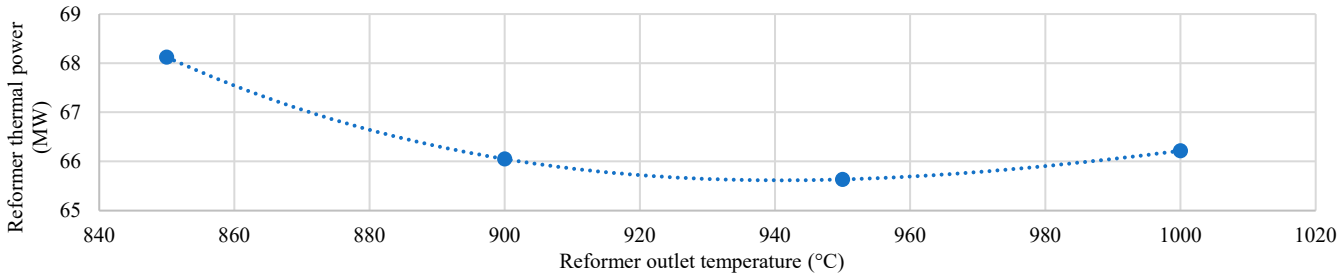

Figure 7. Thermal power vs. reformer outlet temperature.

Ultimately, as the reformer inlet temperature increases, the fuel HUF in the SMR process with air combustion was 8.1% lower than that in the SMR process with oxygen combustion (Figure 8). This is mostly due to the difference in the pressure drop in the air compressor and in the CO_2 compressor (in the first case, the pressure increases 20 times, and in the second, 1.05 times), which leads to a significant difference in the auxiliary electric power consumption. Factoring in the energy consumption, the air separation consumption during oxy-fuel combustion was proven to be 2.3 times lower, as shown in Figure 9.

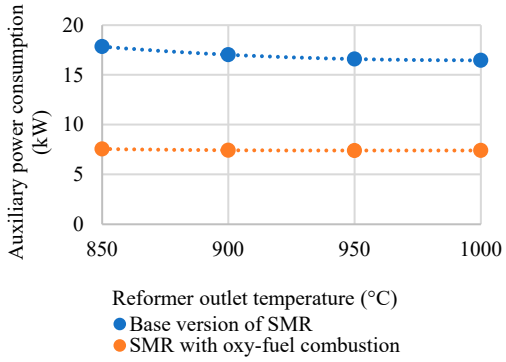

(**a**) Auxiliary power consumption

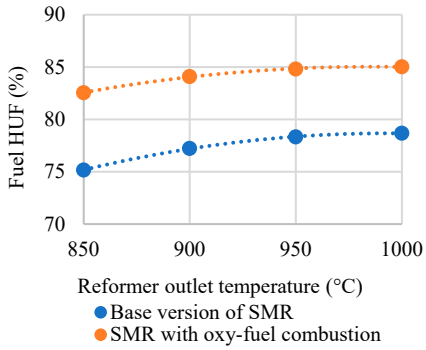

(**b**) SMR fuel HUF

Figure 8. Energy indicators for SMR.

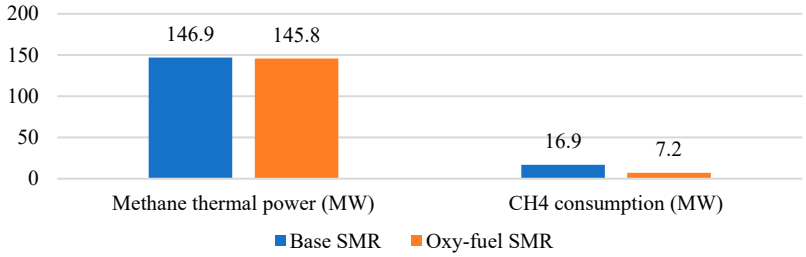

(**a**) Change in the energy consumption SRM

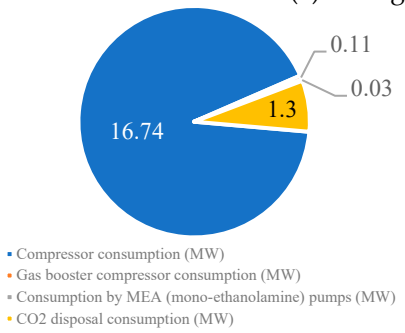

(**b**) Air-fuel combustion

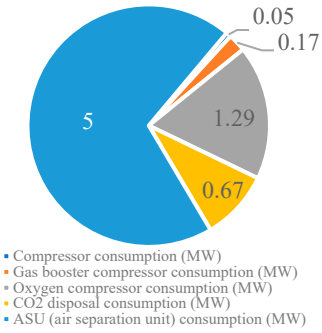

(**c**) Oxy-fuel combustion

Figure 9. Thermal and electrical energy consumption during SRM operation.

In addition to higher efficiency, the SMR process with oxygen fuel combustion results in a 22-fold reduction in carbon dioxide emissions per 1 kg of H_2 produced, as evidenced by the data in Table 5.

Table 5. Simulation results.

Value	Parameter	
Oxidizer	**Air**	**Oxygen**
Fuel mass flow in SMR, kg/s	2.39	2.39
Fuel mass flow in CC, kg/s	0.49	0.78
Hydrogen mass flow, kg/s	1.00	1.00
Air/carbon dioxide compressor power, kW	16,735.03	49.57
Fuel compressor power, kW	106.26	165.31
Oxygen compressor power, kW	-	1285.23

Table 5. *Cont.*

Value	Parameter	
Oxidizer	**Air**	**Oxygen**
Monoethanolamine pumps power, kW	5.53	-
	20.24	-
CO_2 storage power, kW	1304.25	670
ASU cost, kW	-	4999.44
Reboiler power, kW	14,442.78	670
CO_2 capture, %	89.1	99
Fuel HUF, %	76.10	84.25

3. Research and Development of a Novel Oxy-Fuel Combustion Power Cycle for Electricity and Hydrogen Production

3.1. Technological Scheme of the Prospective Oxy-Fuel Combustion Power Cycle

Among oxy-fuel cycles, the SCOC-CC cycle has the simplest configuration [33]. It is a semi-closed oxy-fuel gas turbine cycle that involves the recovery of heat from the CO_2 turbine exhaust gases in a waste heat boiler that generates steam for a steam turbine plant (Figure 10).

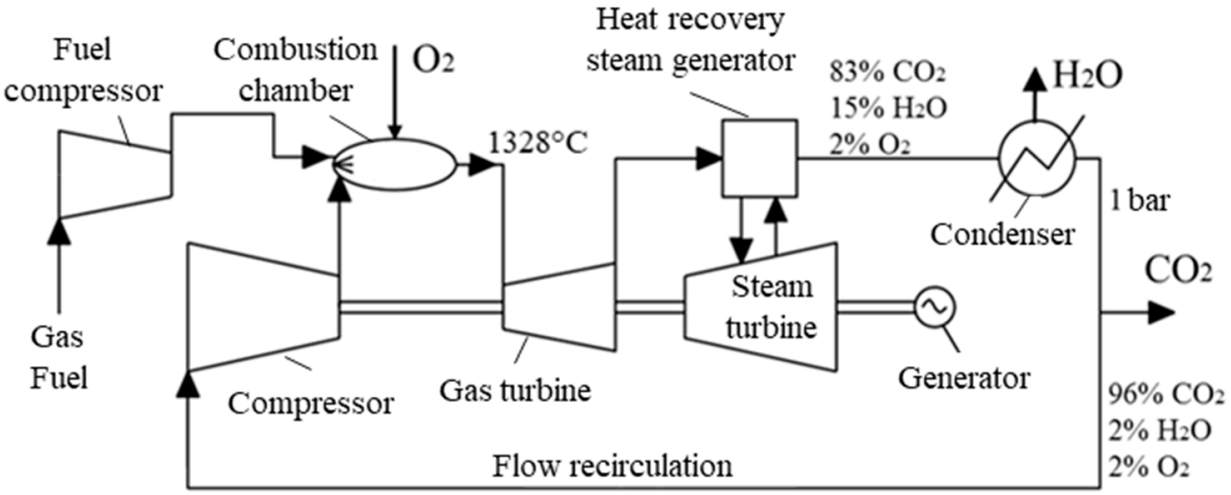

Figure 10. Thermal scheme for the SCOC-CC cycle.

Figure 11 shows the process flow diagram developed for an oxy-fuel energy complex for the combined production of electricity and hydrogen with zero harmful emissions. Table 6 summarizes the input data used for building the power unit model.

3.2. Mathematical Model of the Prospective Oxy-Fuel Combustion Power Cycle

The thermodynamic parameters of the SCOC–CC combined cycle with steam reforming of methane were taken from the REFPROP database. Mathematical modeling of the developed cycle was carried out in the Aspen Plus mathematical package [31,32].

During modeling, the power unit was divided into the oxy-fuel power unit and the steam methane reformer, as shown in Figure 12.

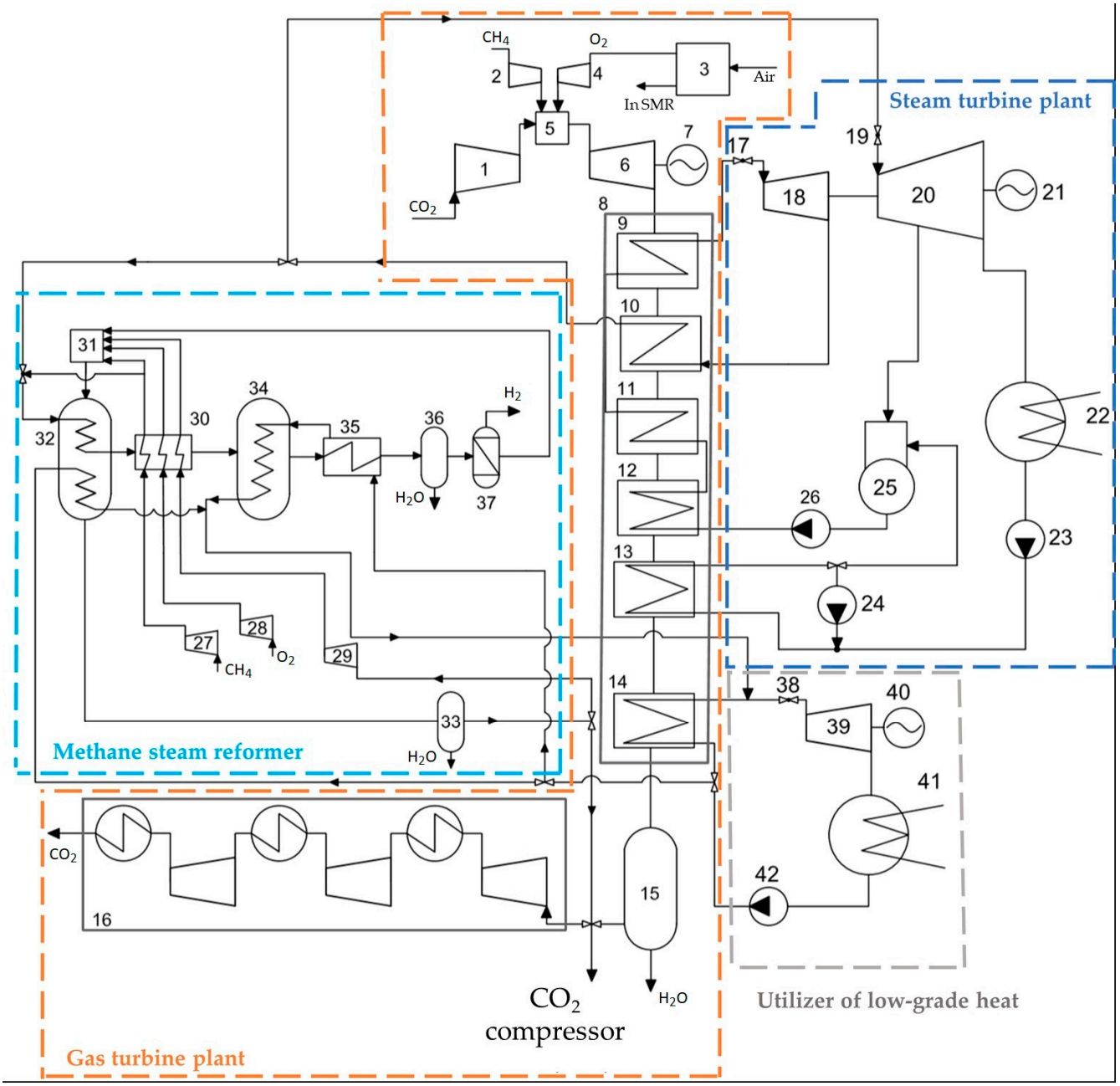

Figure 11. Process flow diagram of the oxy-fuel energy complex for the combined production of electricity and hydrogen: (1) multi-stage CO_2 compressor; (2) gas booster compressor; (3) ASU; (4) O_2 compressor; (5) combustion chamber; (6) CO_2 turbine; (7) first power generator; (8) waste heat boiler; (9) steam superheater; (10) intermediate superheater; (11) evaporating surface; (12) economizer; (13) gas-fueled condensate heater; (14) low-grade heat exchanger; (15) first cooler/separator; (16) disposal compressor; (17) first throttle; (18) HP turbine; (19) second throttle; (20) LP and MP turbines; (21) second power generator; (22) condenser; (23) condensate pump; (24) recirculation pump; (25) deaerator; (26) feed pump; (27) SMR gas booster compressor; (28) SMR O_2 compressor; (29) SMR CO_2 compressor; (30) multiflow WHE; (31) reformer furnace; (32) reformer; (33) second cooler/separator; (34) high-temperature CO conversion reactor; (35) heater; (36) third cooler/separator; (37) variable pressure adsorber; (38) third throttle; (39) CO_2 turbine; (40) third electric generator; (41) CO_2 condenser; (42) CO_2 pump.

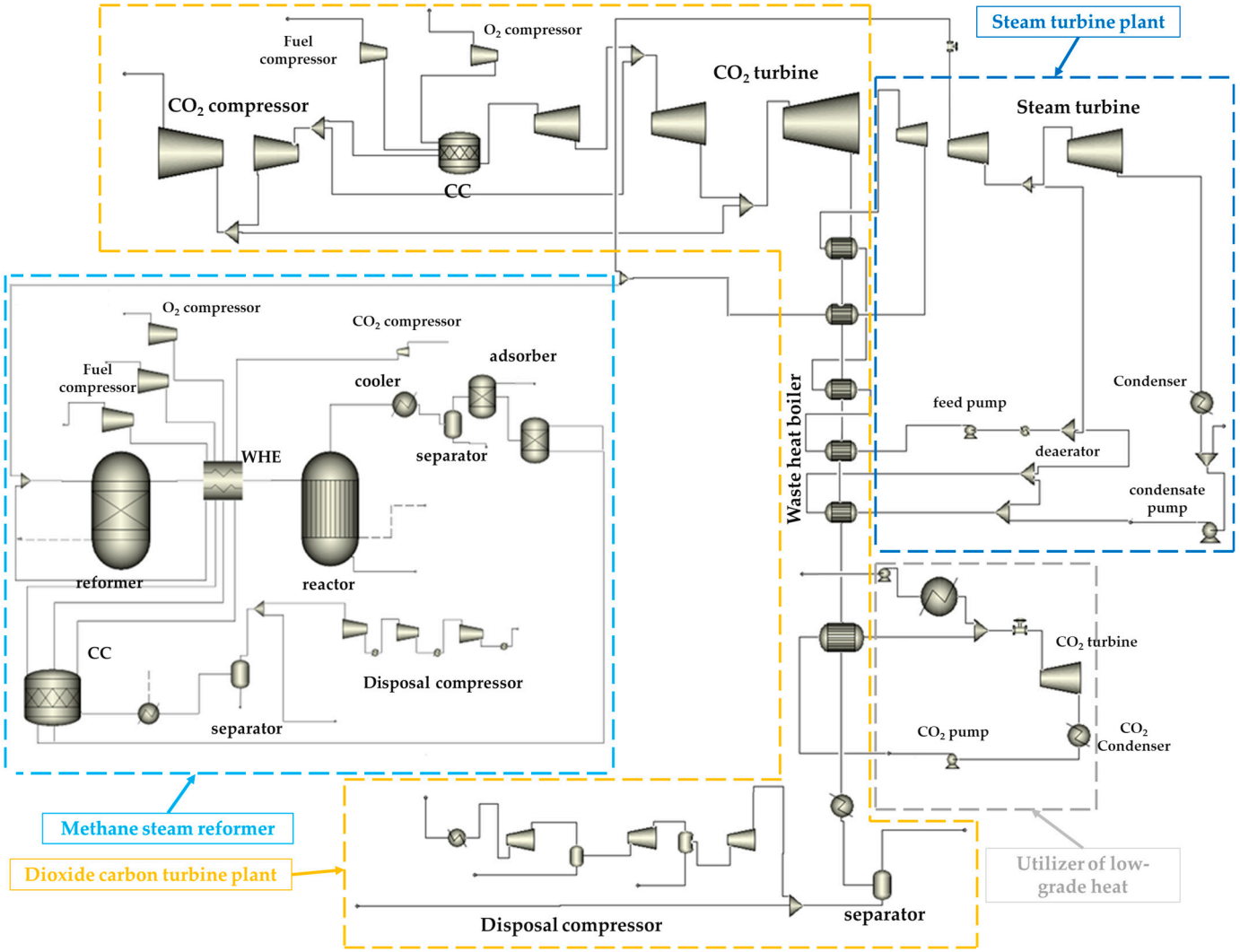

Figure 12. Mathematical model of an oxy-fuel combustion power plant with steam reforming of methane.

Formula (5) was used to calculate the gross power generation for the developed power unit configuration:

$$N_{pc}^{g} = N_{gtp} + N_{stp} + N_{tr} \quad (5)$$

where N_{gtp} is the gross power generation by the gas turbine plant, taking into account the internal efficiency;

N_{stp} is the gross power generation by steam turbine plant, taking into account the internal efficiency;

N_{tr} is the gross power generation by the turbine that recycles low-grade heat, taking into account the internal efficiency.

Formula (6) was used to calculate the power consumed for the own needs for the developed power unit configuration:

$$N_{o.n.pc} = N_{o.n.gtp} + N_{o.n.stp} + N_{o.n.tr} \quad (6)$$

where $N_{o.n.gtp}$ is the power consumed for the own needs of the gas turbine plant;

$N_{o.n.stp}$ is the power consumed for the own needs of the steam turbine plant;

$N_{o.n.tr}$ is the power consumed for the own needs of a turbine that that recycles low-grade heat.

Table 6. Assumptions used in cycle simulations.

No.	Characteristics	Value
1	Lower heating value for CH_4, kJ/kg	50,025
2	Fuel temperature, °C	15
3	Fuel pressure, bar	7
4	Fuel compressor isentropic/mechanical efficiency, %	80/99
5	Mechanical efficiency, %	99
6	Generator electricity/mechanical efficiency, %	98.5/99.4
7	Combustor pressure drop, %	4
8	Minimum cycle temperature, °C	30
14	CO_2 turbine inlet mass flow, kg/s	100
15	HP steam temperature °C	560
	HP steam pressure, MPa	14
16	LP steam pressure, bar	7
17	Condenser pressure in steam turbine unit, bar	0.045
18	Deaerator operating pressure, bar	1.21
19	Steam turbine polytropic efficiency, %	89
20	Pump polytropic efficiency, %	70
22	Gas pressure drop in the heat recovery steam generator, Pascal	100
23	HP superheater minimum pinch, °C	20
24	ASU power consumption, kW/(kg/s)	900
25	O_2 purity, %	91.25
29	Condenser efficiency	0.8
	Ambient temperature, °C	15
	Ambient pressure, bar	1.013

Formula (7) was used to estimate the efficiency of the oxy-fuel power complex with SMR:

$$\eta_{pc}^{net} = \frac{N_{pc}^{g} - N_{o.n.pc}}{B_{pc} \cdot Q_{l_{\mathrm{CH4}}}^{h}} \quad (7)$$

where B_{pc} is the methane consumption by the combustion chamber of the oxy-fuel power complex with SMR.

Since the simulation of SCOC-CC processes with SMR involves generation of electrical energy and hydrogen, the fuel heat utilization factor calculated using Formula (8) was used as the main indicator of their energy efficiency:

$$Fuel\ HUF = \frac{G_{\mathrm{H_2}} \cdot Q_{l_{\mathrm{H2}}}^{h} - \frac{N_{o.n.\ MSR} + N_{capt.MSR} + N_{storage}}{\eta_{elect.}} + N_{pc}^{g} - N_{o.n.pc}}{B_{MSR} \cdot Q_{l_{\mathrm{CH4}}}^{h} + B_{pc} \cdot Q_{l_{\mathrm{CH4}}}^{h}} \quad (8)$$

3.3. Thermodynamic Analysis the Prospective Oxy-Fuel Combustion Power Cycle

Initially, a thermodynamic analysis of the effect of the amount of hydrogen produced on the energy efficiency of the developed oxy-fuel energy complex with steam methane reforming was performed with a constant flow rate of methane fed to the combustion chamber. Within the framework of the study, three cases were examined: the power plant operating in the condensing mode without hydrogen production (Case A), the mode with the production of 4 kg H_2/s (Case B), and the mode with the production of 8 kg H_2/s (Case C). The simulation data (Figure 13) established that an increase in the mass flow rate of hydrogen from 0 kg/s to 8 kg/s leads to a 25.4% decrease in the gross power of the power unit, which is due to a decrease in the coolant mass flow rate and throttling pressure losses at the inlet of the medium pressure turbine by 34.7 kg/s and 1.25 MPa, respectively. There is also extra power consumption by auxiliaries, which is required to maintain the operation of the steam methane reformer, causing the electrical power consumption to increase by 90 MW. Furthermore, 32 kg/s more natural gas is supplied to the reformer, due to which the amount of heat supplied into the cycle increases by 1623 MW. It should be noted that the thermal power (8 kg/s) of produced hydrogen yields 1440 MW of usable energy.

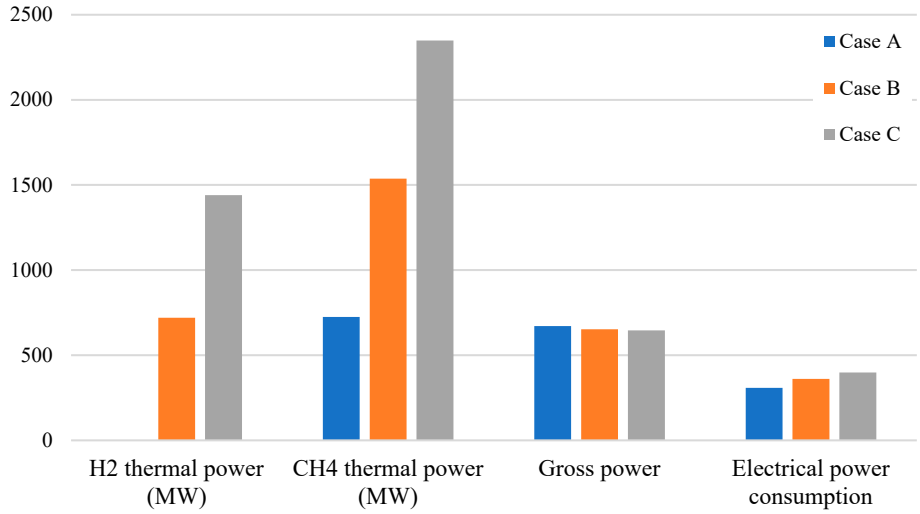

Figure 13. Comparison of the energy performance of an oxy-fuel combustion power plant with steam reforming of methane, with a change in the amount of hydrogen produced.

When switching from the condensing mode to the mode with the combined generation of electrical power and hydrogen, at a constant CO_2 flow rate in the multistage compressor, the power generated by the gas turbine in Case A, Case B, and Case C does not change and remains equal to 533.3 MW; however, electrical power generation by the steam turbine circuit drops by 65 MW. Thanks to the recovery of low-grade heat in the waste heat recovery circuit, the power generated by the CO_2 turbine increases by 39.5 MW. It should be noted that the total generated electric power of the steam turbine cycle decreases by 25.4 MW. The key performance data is provided in Figure 14.

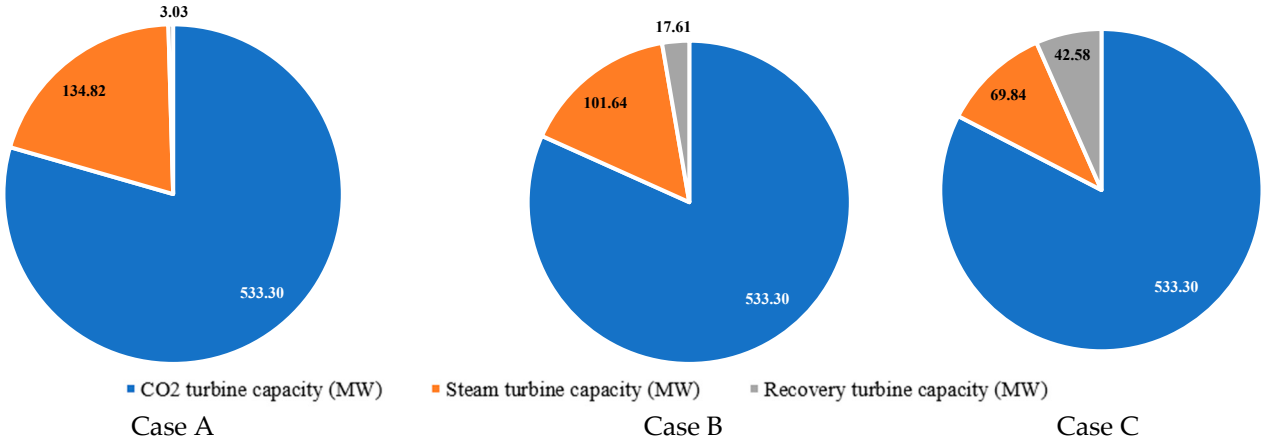

Figure 14. Generated electrical power in the combined power unit.

Figure 15 illustrates the change in auxiliary power consumption when hydrogen production increases from 0 kg/s to 8 kg/s. In Case A, Case B, and Case C, the main electrical energy consumer is the multi-stage CO_2 compressor, consuming 236 MW of power. Percentage-wise, out of the total auxiliary power consumption by the power unit, the multistage CO_2 compressor consumes 76.6% in Case A, 65.4% in Case B, and 59.3% in Case C. This decrease is due to extra power consumption by the SMR gas booster compressor, the SMR O_2 compressor, the SMR ASU, and the SMR CO_2 compressor, the total power of which amounts to 37.8 MW for Case B and 64.9 MW for Case C. One should note that the auxiliary power of the steam turbine cycle at constant capacity of waste heat boiler remains practically the same and equals 1.35 MW.

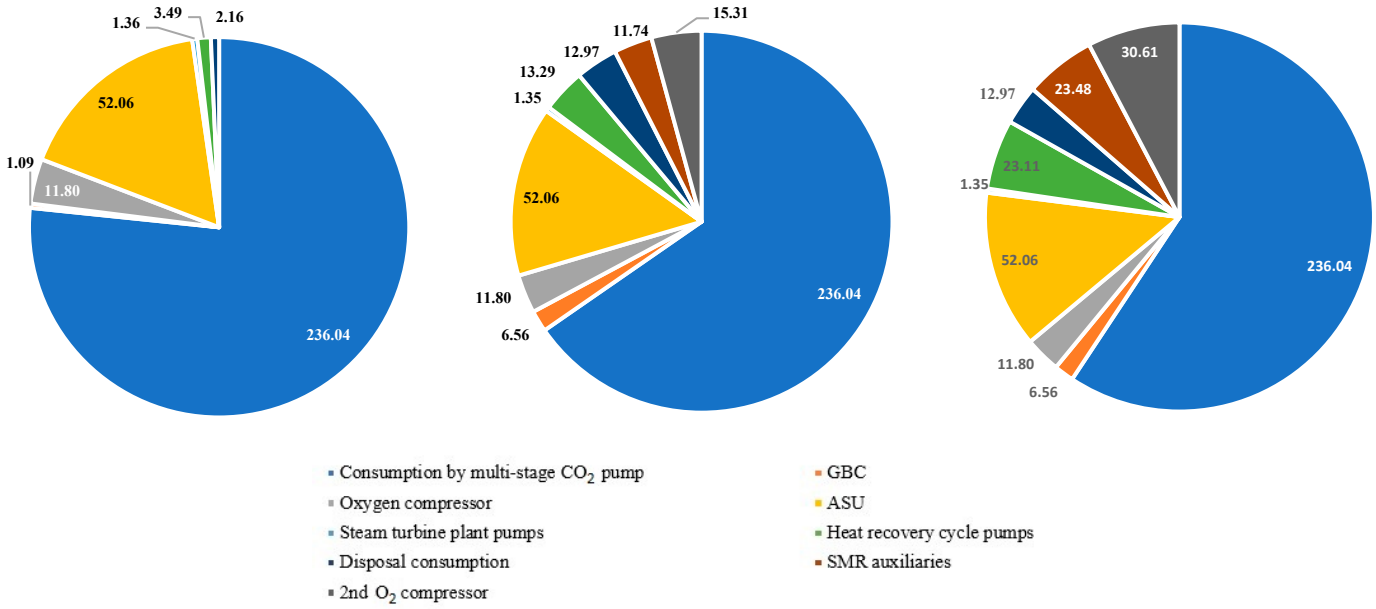

Figure 15. Change in the auxiliary needs of the combined power unit with a change in the generation of H_2.

The power unit energy performance curve is shown in Figure 16. When hydrogen production is increased by 12 kg/s, the net efficiency of the combined power unit drops by 8.8%; this deterioration of efficiency is due to a decrease in the flow rate of the working flow in the MP turbine, which leads to lower electrical power generation and higher pressure losses in the throttling valve. Fuel HUF in the oxy-fuel energy complex with SMR grows by 23.5%. This is due to the energy effect of the combined power and H_2 generation, which reduces the heat loss in the condenser by 79.2 MW.

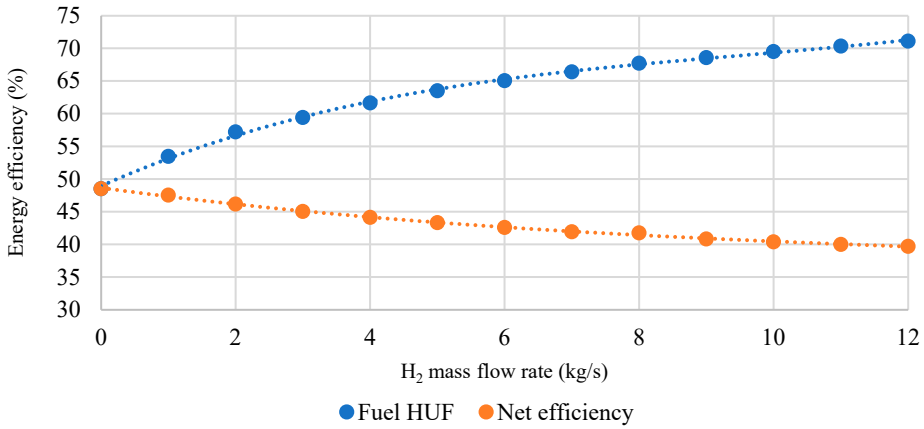

Figure 16. Dependence of the energy efficiency indicators of the power unit on the change in the productivity of the mass flow H_2.

The next step was to conduct an analysis of the energy effect accomplished by the combined production of electrical power and hydrogen compared to separate production; the results are shown in Figure 17. For that purpose, simulations were run to determine the energy performance indicators of the power unit using the SCOC-CC cycle, and the SMR plant per 1 kg of hydrogen produced. The net efficiency of the separate generation has been found to exceed that of the combined generation by 0.67%, which is due to the fact that in the combined generation of electrical power and H_2, a smaller amount of the coolant is able to perform in the MP and LP turbines. However, fuel HUF in the steam methane

reformer in the combined generation of electrical power and H_2 increases by 7.24%. This is due to lower heat supply to the combustion chamber for heating methane and steam entering the reformer.

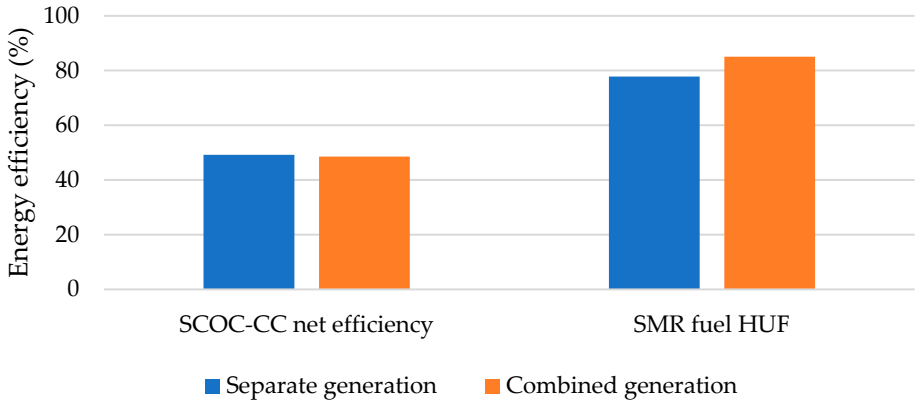

Figure 17. Comparison of energy performance in separate and combined hydrogen production.

The performance of the developed oxy-fuel energy complex will largely depend on the amount of electrical power and hydrogen produced. To simplify the assessment of the key performance indicators in the energy complex, special parameter charts were developed (Figures 18 and 19). The first parameter chart (Figure 18) can be used to determine the net power of the power unit when the amount of hydrogen produced is changed. The second parameter chart (Figure 19) can be used to determine fuel HUF and the net efficiency of the power unit when the amount of hydrogen produced is changed.

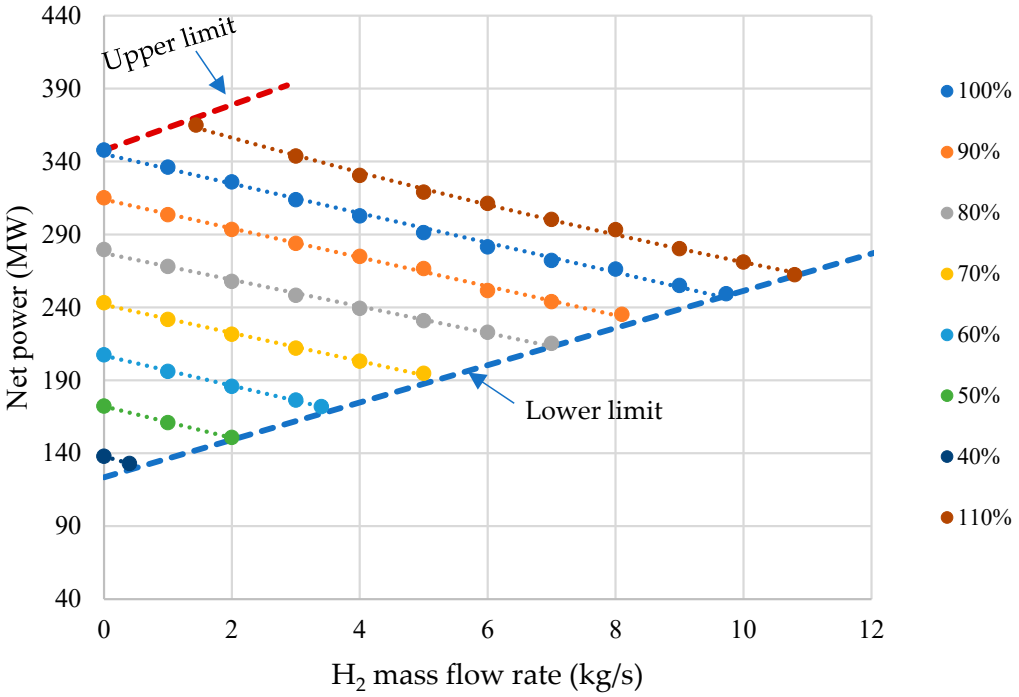

Figure 18. Parameter chart for the power unit capacity.

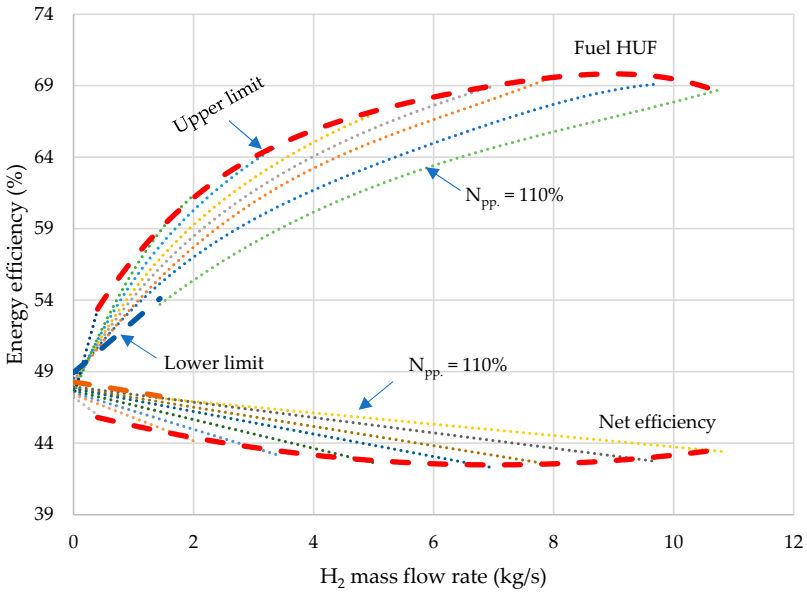

Figure 19. Parameter chart for fuel HUF and the net efficiency of the power unit.

According to the results of thermodynamic analysis of a novel oxy-fuel combustion power cycle, it was found that its performance varies in the range of electricity production (123.6–370 MW) and hydrogen production (0–10.8 kg/s). The efficiency of the oxy-fuel combustion power cycle varies in the range of 47.2–70.1%.

It should be noted that the lower and upper limits of the parameter charts in Figures 18 and 19 are determined by the operating mode of the MP turbine; if the amount of hydrogen produced changes, the mass flow rate of the working flow fed to the steam turbine would also change. The allowable operating range that we have adopted is 110%–40% of the rated load in the MP turbine.

4. Conclusions

This paper presents the following results:

1. In the course of the research, the SMR process with oxy-fuel combustion was found to have a fuel HUF 8.1% higher than in the SMR process with absorption purification of exhaust gases. It also offers the reduction of auxiliary power consumption and CO_2 emissions by 2.3 and 22, respectively. However, the use of pure oxygen and CO_2 at an elevated temperature necessitates the supply of 1.6 times more CH_4 to maintain the temperature in the reformer.
2. The configuration of the hydrogen production process that is based on steam methane reforming with oxy-fuel combustion is a more efficient and environmentally safe solution compared to traditional processes. The SMR process with oxygen fuel combustion achieves a 22-fold reduction in CO_2 emissions per 1 kg of H_2 produced. However, the need for a continuous supply of pure oxygen raises a number of issues and requires a detailed economic analysis to be conducted in further research.
3. The simulation results show that with an increase in the mass flow of hydrogen from 0 to 8 kg/s, the gross power of the power unit decreases by 25.4%. This is mainly due to additional own needs to maintain the operation of the methane steam conversion plant, which is why electricity costs increase by 90 MW.
4. It is established that, as a percentage of all own needs of the energy unit, the energy costs of a multistage carbon dioxide compressor are 76.6% for Case A, 65.4% for Case B, and 59.3% for Case C. This decrease is associated with additional costs for the operation of the SMR gas booster compressor, the SMR O_2 compressor, the SMR ASU, and the SMR CO_2 compressor, the total capacity of which for Case B is 37.8 MW, and for Case C is 64.9 MW.

5. The thermodynamic analysis of the developed oxy-fuel power complex with steam methane reforming showed that with a 12 kg/s increase in hydrogen output, the net efficiency of the combined power unit drops by 8.8%. This effect is due to a decrease in the flow rate of the working flow in the MP turbine, which reduces the electrical power generation and leads to higher pressure losses in the throttling valve. Due to lower losses in the condenser in the combined generation of electricity and H_2, the fuel HUF of the oxy-fuel energy complex with SMR grows by 23.5%.
6. The net efficiency of separate generation has been found to exceed that of combined generation by 0.67%, which is due to the fact that in the combined generation of electrical power and H_2, a smaller amount of the coolant is able to perform in the MP and LP turbines. However, fuel HUF of the steam methane reformer in the combined generation of electrical power and H_2 increases by 7.24%. This is due to lower heat supply to the combustion chamber for heating methane and steam entering the reformer.
7. Parameter charts have been developed as the tools for determining the net power, HUF, and net efficiency with changes in generation of electricity and H_2 by the gas turbine. The study has shown that the capacity of an oxy-fuel plant with steam methane reforming ranges from 123.6 to 370.0 MW, the power unit's hydrogen output is 0–10.8 kg/s, while the fuel heat utilization factor varies within the range of 47.2–70.1%.

Author Contributions: Conceptualization, V.K.; methodology, V.K.; software, D.K. and M.O. (Mikhail Ostrovsky); validation, M.O. (Maksim Oparin) and D.K.; formal analysis, A.R.; investigation, M.O. (Maksim Oparin) and D.K.; resources, D.K.; data curation, M.O. (Mikhail Ostrovsky); writing—original draft preparation, M.O. (Maksim Oparin); writing—review and editing, A.R.; visualization, M.O. (Mikhail Ostrovsky); supervision, V.K.; project administration, V.K.; funding acquisition, A.R. All authors have read and agreed to the published version of the manuscript.

Funding: The investigation has been carried out within the framework of the project "Development of advanced energy complexes for the production of electricity and hydrogen with minimal emissions of hazardous substances into the atmosphere", with the support of a subvention from the National Research University "MPEI" for implementation of the internal research program "Priority 2030: Future Technologies" in 2022–2024.

Conflicts of Interest: The authors declare no conflict of interest.

References

1. Lisin, E.; Kurdiukova, G.; Okley, P.; Chernova, V. Efficient Methods of Market Pricing in Power Industry within the Context of System Integration of Renewable Energy Sources. *Energies* **2019**, *12*, 3250. [CrossRef]
2. Rogalev, N.; Sukhareva, E.; Mentel, G.; Brozyna, J. Economic Approaches for Improving Electricity Market. *Terra Econ.* **2018**, *16*, 140–149.
3. Atkinson, A.; Messy, F.A. Measuring Financial Literacy: Results of the OECD/International Network on Financial Education (INFE) Pilot Study. 2012. Available online: https://www.oecd-ilibrary.org/finance-and-investment/measuring-financial-literacy_5k9csfs90fr4-en (accessed on 8 February 2023).
4. Litvinenko, V.; Tcvetkov, P.; Dvoynikov, M.; Buslaev, G. Barriers to Implementation of Hydrogen Initiatives in the Context of Global Energy Sustainable Development. *J. Min. Inst.* **2020**, *244*, 428–438. [CrossRef]
5. IE Kopteva, A.; Kalimullin, L.; Tcvetkov, P.; Soares, A. Prospects and Obstacles for Green Hydrogen Production in Russia. *Energies* **2021**, *14*, 718. [CrossRef]
6. Amez, I.; León, D.; Ivannikov, A.; Kolikov, K.; Castells, B. Potential of CBM as an Energy Vector in Active Mines and Abandoned Mines in Russia and Europe. *Energies* **2023**, *16*, 1196. [CrossRef]
7. Staffell, I.; Scamman, D.; Abad, A.V.; Balcombe, P.; Dodds, P.E.; Ekins, P.; Shah, N.; Ward, K.R. The role of hydrogen and fuel cells in the global energy system. *Energy Environ. Sci.* **2019**, *12*, 463–491.
8. Ma, L.C.; Castro-Dominguez, B.; Kazantzis, N.K.; Ma, Y.H. Integration of membrane technology into hydrogen production plants with CO_2 capture: An economic performance assessment study. *Int. J. Greenh. Gas Control* **2015**, *42*, 424–438.
9. Anantharaman, R.; Jordal, K.; Roussanaly, S.; Fu, C.; Wahl, P.E.; Brakstad, E.; Riboldi, L.; Gilardi, C.; Clapis, A.; Mancuso, L.; et al. Understanding the cost of retrofitting CO_2 capture to an integrated oil refinery. In Proceedings of the 14th International Conference on Greenhouse Gas Control Technologies, GHGT-14, Leeds, Melbourne, Australia, 21–25 October 2018; 6p.

10. Collodi, G.; Azzaro, G.; Ferrari, N.; Santos, S.; Brown, J.; Cotton, B.; Lodge, S. IEAGHG,"Techno-Economic Evaluation of SMR Based Standalone (Merchant) Plant with CCS", 2017/02, February 2017. Available online: https://ieaghg.org/exco_docs/2017-02.pdf (accessed on 8 February 2023).
11. Yun, J.; Cho, K.; Lee, Y.D.; Yu, S. Four different configurations of a 5 kW class shell-and-tube methane steam reformer with a low-temperature heat source. *Int. J. Hydrogen Energy* **2018**, *9*, 4546–4562. [CrossRef]
12. Descamps, C.; Bouallou, C.; Kanniche, M. Efficiency of an Integrated Gasification Combined Cycle (IGCC) power plant including CO_2 removal. *Energy* **2008**, *6*, 874–881. [CrossRef]
13. Raksajati, A.; Ho, M.T.; Wiley, D.E. Reducing the cost of CO_2 capture from flue gases using aqueous chemical absorption. *Ind. Eng. Chem. Res.* **2013**, *47*, 16887–16901. [CrossRef]
14. Chen, W.; Zhang, G.; Li, B.; Liu, M.; Liu, J. Simulation study on 660 MW coal-fired power plant coupled with a steam ejector to ensure NOx reduction ability. *Appl. Therm. Eng.* **2017**, *111*, 550–561. [CrossRef]
15. Sohn, J.; Hwang, I.S.; Hwang, J. Improvement of ammonia mixing in an industrial scale selective catalytic reduction De-NOx system of a coal-fired power plant: A numerical analysis. *Process Saf. Environ. Prot.* **2021**, *147*, 334–345.
16. Ma, T.; Takeuchi, K. Technology choice for reducing NOx emissions: An empirical study of Chinese power plants. *Energy Policy* **2017**, *102*, 362–376. [CrossRef]
17. Dutta, R.; Nord, L.O.; Bolland, O. Selection and design of post-combustion CO_2 capture process for 600 MW natural gas fueled thermal power plant based on operability. *Energy* **2017**, *121*, 643–656. [CrossRef]
18. Mahmoudi, R.; Emrouznejad, A.; Khosroshahi, H.; Khashei, M.; Rajabi, P. Performance evaluation of thermal power plants considering CO_2 emission: A multistage PCA, clustering, game theory and data envelopment analysis. *J. Clean. Prod.* **2019**, *223*, 641–650. [CrossRef]
19. Kindra, V.O.; Milukov, I.A.; Shevchenko, I.V.; Shabalova, S.I.; Kovalev, D.S. Thermodynamic analysis of cycle arrangements of the coal-fired thermal power plants with carbon capture. *Arch. Thermodyn.* **2021**, *42*, 103–121.
20. Kanniche, M.; Le Moullec, Y.; Authier, O.; Hagi, H.; Bontemps, D.; Neveux, T.; Louis-Louisy, M. Up-to-date CO_2 Capture in Thermal Power Plants. *Energy Procedia* **2017**, *114*, 95–103. [CrossRef]
21. Peng, J.; Yu, B.-Y.; Liao, H.; Wei, Y.-M. Marginal abatement costs of CO_2 emissions in the thermal power sector: A regional empirical analysis from China. *J. Clean. Prod.* **2018**, *171*, 163–174.
22. Hong, J.; Chaudhry, G.; Brisson, J.G.; Field, R.; Gazzino, M.; Ghoniem, A.F. Analysis of oxy-fuel combustion power cycle utilizing a pressurized coal combustor. *Energy* **2009**, *34*, 1332–1340.
23. Kindra, V.; Rogalev, A.; Zlyvko, O.; Sokolov, V.; Milukov, I. Research and development of a high-performance oxy-fuel combustion power cycle with coal gasification. *Arch. Thermodyn.* **2021**, *42*, 155–168.
24. Kindra, V.; Osipov, S.; Zlyvko, O.; Shcherbatov, I.; Sokolov, V. Thermodynamic analysis of an innovative steam turbine power plant with oxy-methane combustors. *Arch. Thermodyn.* **2021**, *42*, 123–140.
25. Barba, F.C.; Sanchez, G.M.D.; Segui, B.S.; Darabkhani, H.G.; Anthony, E.J. A technical evaluation, performance analysis and risk assessment of multiple novel oxy-turbine power cycles with complete CO_2 capture. *J. Clean. Prod.* **2016**, *133*, 971–985. [CrossRef]
26. Allam, R.; Martin, S.; Forrest, B.; Fetvedt, J.; Lu, X.; Freed, D.; Brown, G.W.; Sasaki, T.; Itoh, M.; Manning, J. Demonstration of the Allam Cycle: An update on the development status of a high efficiency supercritical carbon dioxide power process employing full carbon capture. *Energy Procedia* **2017**, *114*, 5948–5966.
27. Zhang, N.; Lior, N. Two novel oxy-fuel power cycles integrated with natural gas reforming and CO_2 capture. *Energy* **2008**, *33*, 340–351. [CrossRef]
28. Ahn, J.H.; Jeong, J.H.; Choi, B.S.; Kim, T.S. Influence of various carbon capture technologies on the performance of natural gas-fired combined cycle power plants. *J. Mech. Sci. Technol.* **2019**, *33*, 1431–1440.
29. Kindra, V.; Zlyvko, O.; Zonov, A.; Kovalev, D. An Oxy-Fuel Power Plant for Hydrogen Production with Near-Zero Emissions. In *SMART Automatics and Energy: Proceedings of SMART-ICAE 2021*; Springer Nature Singapore: Singapore, 2022; pp. 291–301.
30. Rogalev, A.; Rogalev, N.; Kindra, V.; Zlyvko, O.; Vegera, A. A study of low-potential heat utilization methods for oxy-fuel combustion power cycles. *Energies* **2021**, *14*, 3364. [CrossRef]
31. Peshev, D.; Livingston, A.G. OSN Designer, a tool for predicting organic solvent nanofiltration technology performance using Aspen One, MATLAB and CAPE OPEN. *Chem. Eng. Sci.* **2013**, *104*, 975–987. [CrossRef]
32. Galashov, N.; Tsibulskiy, S.; Serova, T. Analysis of the Properties of Working Substances for the Organic Rankine Cycle Based Database "REFPROP". *EPJ Web Conf.* **2016**, *110*, 01068. [CrossRef]
33. Bălănescu, D.-T.; Homutescu, V.-M. Performance analysis of a gas turbine combined cycle power plant with waste heat recovery in Organic Rankine Cycle. *Procedia Manuf.* **2019**, *32*, 520–528.
34. Fahim, M.A.; Al-Sahhaf, T.A.; Elkilani, A. *Fundamentals of Petroleum Refining*; Elsevier: Amsterdam, The Netherlands, 2009.